JACS
JOURNAL OF THE AMERICAN CHEMICAL SOCIETY
Article
pubs.acs.org/JACS

1,3-Bis(nitroimido)-1,2,3-triazolate Anion, the *N*-Nitroimide Moiety, and the Strategy of Alternating Positive and Negative Charges in the Design of Energetic Materials

Thomas M. Klapötke,*[,†,‡] Christian Petermayer,[†] Davin G. Piercey,[†] and Jörg Stierstorfer[†]

[†]Department of Chemistry, Energetic Materials Research, Ludwig-Maximilian University of Munich, Butenandstr. 5−13, D-81377 Munich, Germany

[‡]Center for Energetic Concepts Development, CECD, University of Maryland, UMD, Department of Mechanical Engineering, College Park, Maryland 20742, United States

Supporting Information

ABSTRACT: This unique study reports on the 1,3-bis(nitroimido)-1,2,3-triazolate anion. This compound provides unique insight into both academic and practical considerations surrounding high-nitrogen systems. The bonding in this energetic anion can be represented multiple ways, one of which includes a chain of alternating positive/negative charges nine atoms long. The validity of this resonance structure is discussed in terms of experimental, computational, and valence bond results. The prepared materials based on this energetic anion were also characterized chemically (infrared, Raman, NMR, X-ray) and as high explosives in terms of their energetic performances (detonation velocity, pressure, etc.) and sensitivities (impact, friction, electrostatic), and the 1,3-bis(nitroimido)-1,2,3-triazolate anion is found to be very high performing with high thermal stabilities while being quite sensitive to mechanical stimuli.

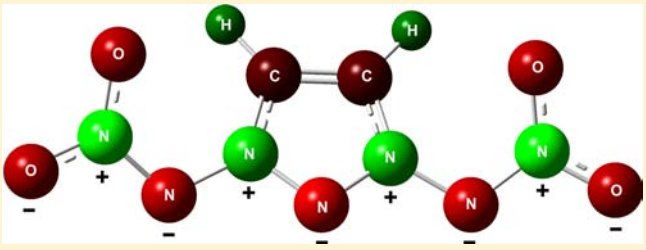

INTRODUCTION

The main challenge in energetic materials chemistry (all of propellants, explosives, and pyrotechnics) is producing a material that will release large amounts of energy when desired but still be safe enough to handle without energetic decomposition.[1−5] Beyond their practical applications, working with such materials on the borderline of existence and nonexistence allows insight into base properties affecting molecular stability and energy capacity. The practical aspect of energetic materials research is focused on ever higher performing explosives and propellants,[6] energetics that can be used with greatly reduced toxicological or environmental results,[7] and materials with increased margins of safe handling.[8] However, on the molecular level, new insights are necessary to determine methods of ever increasing the energy content while retaining stability.

There are two major strategies for incorporating energetic properties into a molecule, and naturally, they can be combined. The first is simply fuel and oxidizer in the same molecule as is seen in quintessential explosives such as TNT (2,4,6-trinitrotoluene) and RDX (1,3,5-trinitro-1,3,5-triazinane). The second broad category is high heat of formation compounds where high heats of formation are created from either highly strained bonds in the molecule (e.g., cubane energetics)[9] or the driving force of a nitrogen-rich compound toward forming nitrogen gas (e.g., 1,1′-azobi-1,2,3-triazole).[10] Unfortunately, these strategies all appear to have limits. In the case of combining fuel and oxidizer in the same molecule using aromatic and aliphatic nitro compounds and nitramines, as the oxygen balance (indicator of ratio of fuels (C,H) to oxidizers (O) in an energetic molecule) improves, the sensitivities toward impact have been shown to increase.[11] A similar effect is seen with high heat of formation compounds: when the five-membered azoles from pyrazole to pentazole are considered, as nitrogen content increases, thermal stability decreases (heat of formation concurrently increases), culminating in the pentazole ring, derivatives of which are not stable at ambient conditions.[12] In the case of heavily strained compounds, octanitrocubane has been prepared; however, the synthesis is exceedingly long, precluding use.[13]

Unlike energetic design strategies based on fuel and oxidizer or strained compounds, nitrogen-rich compounds offer some unique chemical properties that can allow stabilization via several distinct methods. One of the reasons high nitrogen systems that possess extended nitrogen chains are not stable, while the corresponding carbonaceous version is stable, is a result of the lone pair of electrons on the nitrogen atoms. While a nitrogen atom can be considered isoelectronic to a CH group, nitrogen's lone pair possesses electron density which can donate into adjacent σ^* orbitals destabilizing the system.[14] This is the reason that materials such as hexazine (cyclic-N_6) are not

Received: October 30, 2012
Published: November 28, 2012

   dx.doi.org/10.1021/ja310384y | J. Am. Chem. Soc. 2012, 134, 20827−20836

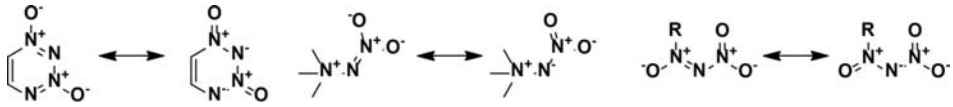

Figure 1. Nitrogen−oxygen APNC systems.

stable. The successful design of such nitrogen-rich systems must adequately separate σ- and π-systems.[15] Tailoring of the molecular shape can achieve this. In the case of the nitrohydrazines, a class of compounds generally regarded to be of low stability, Tartakovsky[16] prepared a bicyclic nitrohydrazine of increased stability where the cis-fixed β-nitrogen lone pair does not possess the flexibility to reach an antiperiplanar arrangement relative to the N−NO_2 bond, a requirement to destabilize the system. Naturally, the placement of electron-withdrawing substituents on the β-nitrogen of a nitrohydrazine was also shown by Tartakovsky to increase the stability of the species,[17] and a similar effect was seen by delocalization when the β-nitrogen was part of a heterocycle, preferably where the heterocyclic nitrogen can be assigned a formal positive charge.[16] In the case of a heterocycle, where ring shape is fixed, σ and π separation can be achieved by functionalization. This is best exemplified by the fully unsaturated 1,2,3,4-tetrazine ring; without ring nitrogen atoms substitution, it is unstable, with only one low-decomposing example of one such compound existing.[18,19] In the case of the 1,2,3,4-tetrazine-1-oxides, an increase in stability is seen with many benzo-annulated species known.[20] The major increase in stability is seen with the 1,2,3,4-tetrazine-1,3-dioxides; generally, members of this class of compounds decompose above 200 °C.[20−22] This increase in stability can be described by the above separation of σ and π systems;[15] however, qualitatively it gives rise to the unique "alternating positive negative charge" (APNC) theory, whereby stable nitrogen-rich systems can have one of their resonance forms illustrated with positive and negative charges on alternating atoms.[16,23] Unique nitrogen−oxygen systems, beyond 1,2,3,4-tetrazine-1,3-dioxides, can all have their resonance forms illustrated in the APNC form including the nitroimide[24,25] and nitrodiazine oxide[16,26] functionalities (Figure 1). When it is considered that heterocycle stabilization by an oxide results from removal of electron density on alternating nitrogen atoms, there is the potential for heterocycle stabilization by the nitroimide functionality, where extended APNC systems can be created.

In this work, we have chosen to investigate the nitration product of the 1,3-diamino-1,2,3-triazolium cation, 1,3-bis-(nitroimido)-1,2,3-triazolate. When one resonance form is considered (Figure 2), an alternating positive/negative charge

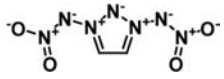

Figure 2. Most charged resonance form of the 1,3-bis(nitroimido)-1,2,3-triazolate anion.

system is created that extends over *nine* atoms when the nitro group resonances are included. This compound was first prepared by Tartakovsky;[27] however, only limited characterization was presented, such as the decomposition point of the potassium salt, and not even a detailed synthesis was presented. In this work we have prepared a variety of energetic salts of the 1,3-bis(nitroimido)-1,2,3-triazolate anion, and these were characterized by X-ray diffraction, infrared and Raman spectroscopy, multinuclear NMR spectroscopy, elemental analysis, and DSC. Computational calculations predicting energetic performance properties confirm the exceedingly high energetic properties of this class of materials. The favorable resonance forms of the APNC system are discussed based on crystallographically determined bond lengths as well as using computational results (NBO and Mulliken charges and valence bond theory). We have exemplarily demonstrated the ability of this unique class of compounds to form energetic materials of high explosive performance and high thermal stability.

RESULTS AND DISCUSSION

Synthesis. The nitration of 1,3-diamino-1,2,3-triazolium nitrate with nitronium tetrafluoroborate is performed at 0 °C for 30 min followed by allowing the solution to warm to room temperature over the next 30 min (Scheme 1). After this time,

Scheme 1. Synthesis of Potassium 1,3-Bis(nitroimido)-1,2,3-triazolate

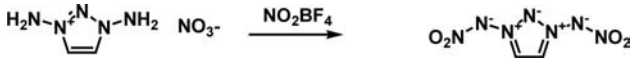

solid potassium acetate is added and the mixture stirred overnight. After filtration of the acetate, acetonitrile is evaporated, and acetic acid is removed as the azeotrope with benzene. Due to the increased solubility of tetrafluoroborate in acetonitrile in the presence of acetic acid, the produced residue was extracted with acetonitrile to obtain crude potassium 1,3-bis(nitroimido)-1,2,3-triazolate (**1**). Raman and ^{19}F NMR confirmed the presence of tetrafluoroborate in the crude material. Crystals were obtained by diffusing ether into a solution of **1** in acetonitrile, and these crystals were used for DSC as well as crystallographic measurement.

The reaction of crude **1** with aqueous silver nitrate solution precipitates the silver salt (**2**) as an off-white solid. Interestingly, when a small sample of high purity **1** from multiple EtOH and MeOH crystallizations is used to prepare the silver salt, the silver salt does not precipitate instantly and instead forms salt-like crystals with dimensions over 1 mm. This crystal growth process is incredibly slow with very tiny crystals visible after a day or two, and 1 mm crystals took over a week. As lower purity samples of **1** were used for the synthesis of **2**, the crystal shape becomes needle-like and finally simply a powder. The powder **2** does not explode but merely deflagrates when ignited, whereas the crystalline material explodes with a very satisfying report when ignited. Due to the high sensitivity of the silver salt, elemental analysis could not be performed to determine purity. Raman measurements were also precluded by the tendency of explosive silver salts to explode upon Raman irradiation.

The silver salt **2** was reacted with ammonium, hydroxylammonium, hydrazinium, and triaminoguanidinium halides to obtain the corresponding energetic salt and silver halide. After filtration of the silver halide and evaporation of the filtrate, the

dx.doi.org/10.1021/ja310384y | J. Am. Chem. Soc. 2012, 134, 20827−20836

ammonium (**3**), hydroxylammonium (**4**), hydrazinium (**5**), and triaminoguanidinium (**6**) salts were isolated, and elemental analysis indicated all were pure. Tetrafluoroborate impurities were assumed to be lost during the precipitation of the silver salt, and only minute traces of tetrafluoroborate were detected in the Raman spectra. All of these salts were crystallized by diffusion of ether into a methanolic solution.

Spectroscopy. The 1,3-bis(nitroimido)-1,2,3-triazolate anion was characterized by proton, carbon-13, and nitrogen-15 NMR in DMSO-d_6. In all salts the lone ^{1}H and ^{13}C signals occur at 8.75 and 129.7 ppm. The ^{15}N spectrum (Figure 3)

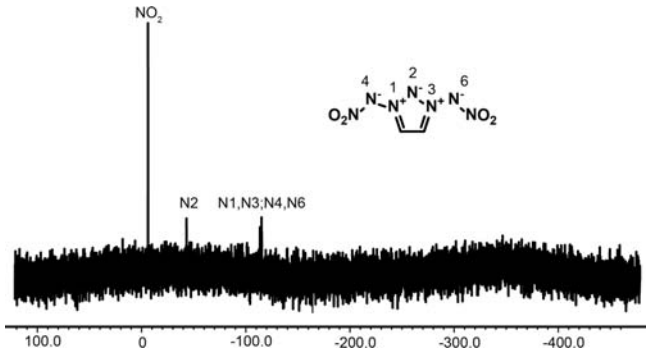

Figure 3. ^{15}N NMR spectrum of the 1,3-bis(nitroimido)-1,2,3-triazolate anion.

possesses four signals, at −6.2, −43.0, −113.6, and −115.3 ppm. Assignments were made based on comparison with a calculated spectrum (MPW1PW91/aug-cc-pVDZ, Gaussian09[28]) where calculated values for N5/N7, N2, N1/N3, and N4/N6 were found to be −12.9, −53.7, −106.2, and −108.7 ppm. These values match well with experimental; however, the difference of N1/N3 and N4/N6 being only 2 ppm in both the experimental and calculated spectra leaves precise assignment of these similar signals ambiguous.

The IR and Raman spectra of all compounds were recorded and assigned using frequency analysis from an optimized structure (B3LYP/cc-pVDZ using the Gaussian 09 software).[28] All calculations were performed at the DFT level of theory; the gradient-corrected hybrid three-parameter B3LYP[29,30] functional theory has been used with a correlation consistent cc-pVDZ basis set.[31−34]

In the Raman spectra, five major bands are observed. The first occurs from 1509 to 1520 cm^{-1} (calcd 1563 cm^{-1}) and results from the NO_2 asymmetric stretch as well as the symmetric triazole C−C ring deformation. The next occurs from 1338 to 1372 cm^{-1} (calcd 1365 cm^{-1}) and results from C1−N1 and C2−N3 triazole symmetric stretch in combination with N1−N4 and N3−N6 stretching. At 1241−1252 cm^{-1} (calcd 1250 cm^{-1}) is the band resultant from C1−C2, N1−N2, and N2−N3 triazole ring breathing. Between 1070 and 1091 cm^{-1} (calcd 1070 cm^{-1}), combined triazole ring breathing with C−H wagging is observed. The final strong band at 1005−1015 cm^{-1} (calcd 1059 cm^{-1}) results from a combination of N−NO_2 stretching and C−H wagging. Traces of tetrafluoroborate impurities (1098, 773, 535, and 359 cm^{-1}) can be seen in several spectra, however, only in trace quantities as evidenced by their intensities and the elemental analyses being correct.

In the literature,[24] nitroimides tend to have two distinct bands from nitro group stretching in the infrared spectrum. The first generally occurs at 1260−1300 cm^{-1} and the next at 1380−1450 cm^{-1}. For the materials prepared, the first of these occurs from 1390 to 1455 cm^{-1} (calcd 1355 cm^{-1}) from N−NO2 symmetric nitro stretching in combination with N1−N2 and N2−N3 asymmetric stretching, while the second (obs. 1244−1280 cm^{-1}, calcd 1310 cm^{-1}) arises from the same vibrations with the addition of asymmetric C−H C−H wagging.

Single Crystal X-ray Structure Analysis. All compounds have been fully characterized by single-crystal X-ray structure determination. Table 1 summarizes a selection of crystallographic data and refinement details. In the literature,[27] mention is made of the structure of potassium salt being known; however, no details were presented. Of interest is the rotational ability of the N2−N3−N6−N7 bond, giving each salt a unique rotation of the "arms" of the nitroimide functionality relative to the triazole ring.

Table 1. Crystallographic Data and Structure Refinement Details for Compounds 1−6

compound	1	2	3	4	5	6
formula	$KC_2H_2N_7O_4$	$AgC_2H_2N_7O_4$	$NH_4C_2H_2N_7O_4$	$NH_4OC_2H_2N_7O_4$	$N_2H_5C_2H_2N_7O_4$	$CN_6H_9C_2H_2N_7O_4$
formula weight [g mol^{-1}]	227.18	295.98	206.15	222.15	221.17	293.25
temperature [K]	173	173	173	173	173	173
crystal system	orthorhombic	orthorhombic	orthorhombic	triclinic	monoclinic	triclinic
space group	$Pca2_1$	$P2_12_12_1$	$Pna2_1$	$P-1$	$P2_1/n$	$P-1$
a [Å]	9.7258 (4)	5.5785(6)	6.4299(2)	5.6251(4)	3.6154(4)	9.6819(14)
b [Å]	19.6056(7)	8.5311(7)	5.6658(2)	7.8446(7)	23.160(2)	9.8267(12)
c [Å]	8.2346(3)	15.4048(11)	20.5491(8)	9.7402(8)	10.0335(9)	12.1787(19)
α [°]	90	90	90	76.794(7)	90	89.446(11)
β [°]	90	90	90	89.114(6)	91.855(11)	88.555(12)
γ [°]	90	90	90	77.979(7)	90	89.845(11)
volume [$Å^3$]	1570.17	733.13(11)	748.61 (5)	409.03(6)	839.69	1158.3(3)
formula Z	8	4	4	2	4	4
space group Z	4	4	4	2	4	4
density calcd [g cm^{-3}]	1.922	2.682	1.829	1.804	1.749	1.683
R_1/wR_2 [all data]	0.0314/0.0643	0.0276/0.0508	0.0395/0.0999	0.0358/0.0725	0.1029/0.1822	0.1243/0.0827
R_1/wR_2 [$I > 2\sigma(I)$]	0.0277/0.0620	0.0238/0.0492	0.0380/0.0978	0.0286/0.0678	0.0714/0.1682	0.0827/0.1990
S	1.044	1.006	1.152	1.050	1.039	1.034
CCDC	905012	905013	905015	905014	905016	905017

dx.doi.org/10.1021/ja310384y | J. Am. Chem. Soc. 2012, 134, 20827−20836

Potassium 1,3-bis(nitroimido)-1,2,3-triazolate (**1**) crystallizes in the orthorhombic space group $Pca2_1$ with four formula units in the unit cell and a density of 1.922 g cm^{-3} (Figure 4). The

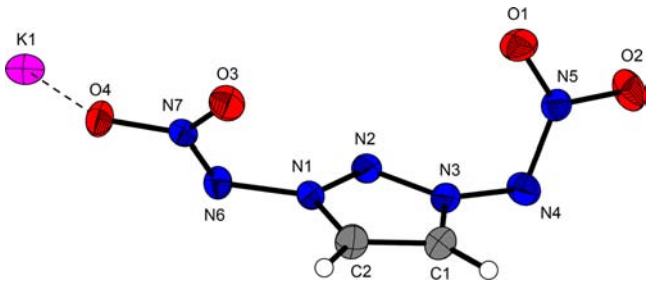

Figure 4. ORTEP representation of the molecular structure of **1**. Displacement ellipsoids are shown at the 50% probability level.

anions are arranged in a wavelike structure along the *b*-axes. The potassium cations are collocated in layers along the *ac*-planes and are coordinated (<3 Å) by the atoms O4, O2, O6, O7, and N6 forming no regular polyhedra.

Silver 1,3-bis(nitroimido)-1,2,3-triazolate (**2**) crystallizes in the orthorhombic space group $P2_12_12_1$ with four formula units in the unit cell and a density of 2.756 g cm^{-3}. (Figure 5) This density is in the range of other silver nitroamino-azoles, e.g., silver 1-methyl-5-nitriminotetrazolate (2.948 g cm^{-3}) in the literature.[35]

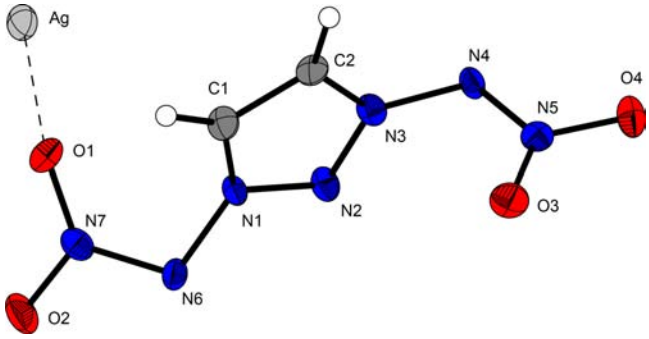

Figure 5. ORTEP representation of the molecular structure of **1**. Displacement ellipsoids are shown at the 50% probability level.

Ammonium 1,3-bis(nitroimido)-1,2,3-triazolate (**3**) crystallizes in the orthorhombic space group $Pna2_1$ with four formula units in the unit cell and a density of 1.829 g cm^{-3} (Figure 6). The structure is strongly influenced by the formation of numerous hydrogen bonds using all ammonium protons, e.g., N8−H8A···O3: 0.82(4), 2.51(4), 3.116(3) Å, 132(4)°; N8−H8D···O4: 0.89(4), 2.37(7), 2.879(3) Å, 116(6)°; N8−H8C···O4^{i}: 0.84(4), 2.35(5), 3.052(4) Å, 142(6)°; and N8−

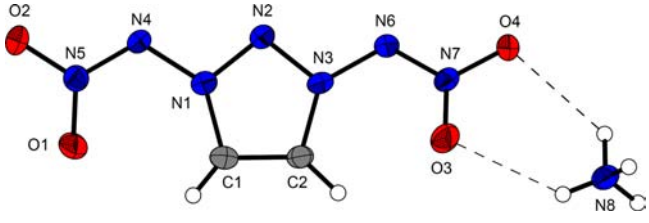

Figure 6. ORTEP representation of the molecular structure of **3**. Displacement ellipsoids are shown at the 50% probability level.

H8B···O2^{ii}: 0.87(4), 2.32(7), 2.957(3) Å, 130(7)° ((i) 0.5 + *x*, −0.5 − *y*, *z*, (ii) −*x*, −*y*, −0.5 + *z*).

Hxdroxylammonium-1,3-bis(nitroimido)-1,2,3-triazolate (**4**) crystallizes in the triclinic space group *P*−1 with two formula units in the unit cell and a density of 1.804 g cm^{-3}. Interestingly this density is lower than that of the ammonium salt **3**, which is usually the other way around. As can be seen from Figure 7, the C connected hydrogen atoms participate in nonclassical hydrogen bonds to the O1^{i} and O3^{i} atoms of a neighbored anion, forming a dimer.

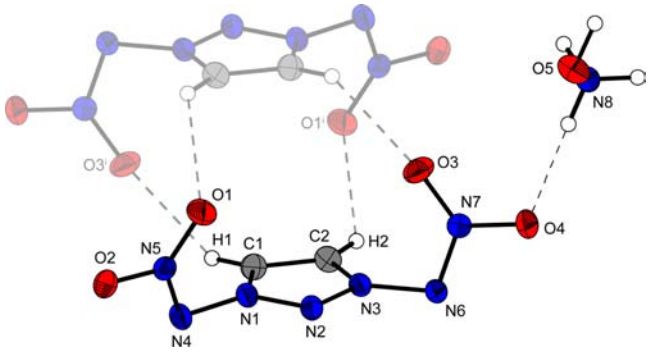

Figure 7. ORTEP representation of the molecular structure of **4** and the formation of nonclassical hydrogen bonds. Displacement ellipsoids are shown at the 50% probability level. Symmetry code: (i) 2 − *x*, −*y*, 1 − *z*.

Hydrazinium-1,3-bis(nitroimido)-1,2,3-triazolate (**5**) crystallizes without inclusion of water or hydrazine in the monoclinic space group $P2_1/n$ with four formula units in the unit cell and a density of 1.749 g cm^{-3} (Figure 8). The anions are arranged in

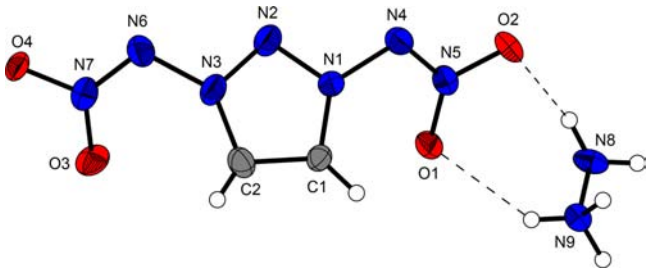

Figure 8. ORTEP representation of the molecular structure of **6**. Displacement ellipsoids are shown at the 50% probability level.

wave-like constitution along the *b*-axes, interrupted by the hydrazinium cations within the *ac*-planes. All hydrogens of the hydrazinium cations participate in hydrogen bonds.

Triaminoguanidinium 1,3-bis(nitroimido)-1,2,3-triazolate (**6**) crystallizes in colorless platelets in the triclinic space group *P*−1 with four formula units in the unit cell. Half of the asymmetric unit is depicted in Figure 9. The density of 1.682 g cm^{-3} is the lowest one observed in this work and can be explained by a relatively loose 3-dim packing (best observable by viewing along the *a* direction). This observed structure was found to be a higher temperature polymorph. Using a PETRAIII synchrotron source at DESY HH with 0.2068A radiation and ranging the sample temperature from 25 K to 300 K, a phase transition was observed at below 170 K.

Table 2 presents selected torsion angles and bond lengths. As the NNO_2 fragments on the compound exhibit a wide range of N2−N1−N4−N5 and N2−N3−N6−N7 torsion angles relative

dx.doi.org/10.1021/ja310384y | J. Am. Chem. Soc. 2012, 134, 20827−20836

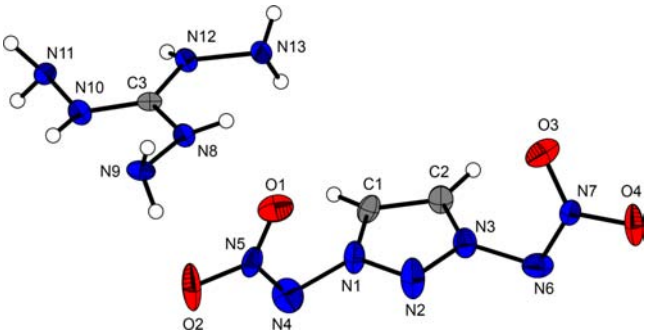

Figure 9. ORTEP representation of the molecular structure of **6**. Displacement ellipsoids are shown at the 50% probability level.

to the triazole ring, the N1−N4 and N3−N6 bonds can reasonably be assumed to be single bonds based on their rotational freedom. In all compounds, this bond length ranges from 1.40 to 1.44 Å, slightly shorter than the standard (1.48) N−N single bond, consistent with the N^+-N^- fragments as seen in pyridine-1-nitroimide where this bond length is seen to be 1.421 Å[36] or in 1-nitroimido-1,2,3-triazole where this bond is 1.40 Å.[37] Interesting to note is that the corresponding bond in the precursor diaminotriazolium cation is also 1.40 Å,[38] again supporting this bond's single nature. As the NNO_2 fragments approach planarity with the ring, we expected to see this bond length decrease due to increased π-system communication; however, this was not seen. The N−N bond lengths within the NNO_2 fragments (N4−N5 and N6−N7) are slightly shorter, ranging from 1.30 to 1.35 Å, approximately half way between a double and single bond, illustrating the contributing nature of the resonance form shown in Figure 10. Within the ring, the bond lengths are comparable to those found in the precursor diaminotriazolium cation.[38]

Computational Structural Considerations. Unfortunately, crystallographic results are not sufficient evidence for the highly charged resonance structure presented in Figure 2, so NBOs (natural bond orbitals) as well as Mulliken charges of the anion were calculated on the B3LYP/cc-PVTZ level of theory using the optimized gas-phase structure with the Gaussian09[28] software (Figure 11).

Figure 10. Contributing double bond resonance form.

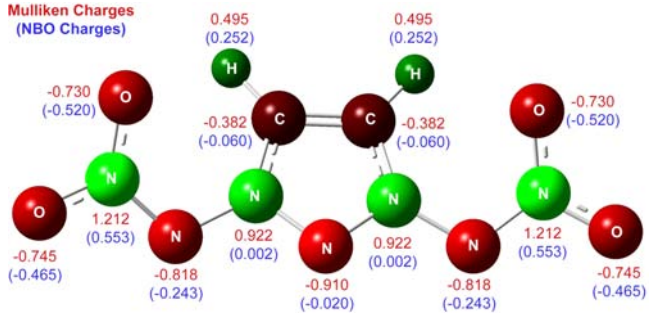

Figure 11. Mulliken and NBO charges on the 1,3-di(nitroimide)-1,2,3-triazolate anion.

First, when the Mulliken charges are considered, a chain of nine atoms with alternating positive and negative charges is seen across the system, exactly what was suggested in Figure 2. NBO charges are considered more reasonable for discussion, and the same trend is seen within the nitroimide functionalities on the 1,2,3-triazole ring; however, within the 1,2,3-triazole ring the charges slightly differ. When NBO charges are considered vs Mulliken, the majority of the triazole ring's negative charge is localized on the carbon atoms in NBO, whereas in Mulliken, the negative charge is located on the central nitrogen atom. The magnitude of the positive charges on the flanking nitrogen atoms is also greatly reduced in NBO charges vs Mulliken; however, when one considers that the triazole ring has negative charge overall, it is unsurprising that formal positive charges would be reduced. Overall, both NBO and Mulliken charges support the contributing nature of the resonance form in Figure 2 in the structure of the 1,3-bis(nitroimido)-1,2,3-triazolate anion.

Next, to judge the contributions of the various resonance forms, we attempted to calculate the contributions of the various resonance forms according to valence bond theory using the program VB2000.[39,40] Unfortunately, the 1,3-

Table 2. Selected Torsion Angles and Bond Lengths

	1	2	3	4	5	6
N2−N1−N4−N5 (°)	−122.9 (2)	−134.0 (3)	160.0 (2)	76.5 (1)	−137.1 (3)	93.3 (5)
° not planar	57.1	46.0	20.0	76.5	42.9	86.7
N2−N3−N6−N7 (°)	82.4 (3)	−93.8 (4)	145.5 (2)	−96.2 (1)	138.5 (3)	−114.6 (5)
° not planar	82.4	86.2	34.5	83.8	41.5	65.4
C1−C2	1.358 (3)	1.351 (5)	1.374 (4)	1.360 (2)	1.368 (6)	1.347 (7)
C1−N1	1.355 (3)	1.349 (5)	1.368 (3)	1.349 (2)	1.363 (5)	1.350 (6)
C2−N3	1.357 (3)	1.351 (5)	1.358 (3)	1.357 (2)	1.373 (5)	1.366 (6)
N1−N2	1.323 (3)	1.323 (4)	1.331 (3)	1.327 (2)	1.323 (4)	1.323 (6)
N2−N3	1.322 (3)	1.328 (4)	1.329 (3)	1.324 (2)	1.330 (4)	1.313 (6)
N1−N4	1.402 (3)	1.404 (4)	1.402 (3)	1.400 (2)	1.403 (4)	1.435 (6)
N3−N6	1.406 (3)	1.397 (5)	1.400 (3)	1.406 (2)	1.441 (5)	1.438 (6)
N4−N5	1.327 (3)	1.349 (5)	1.316 (3)	1.327 (2)	1.341 (4)	1.309 (6)
N6−N7	1.334 (3)	1.338 (5)	1.324 (3)	1.332 (2)	1.298 (4)	1.307 (5)
N5−O1	1.248 (3)	1.241 (4)	1.259 (3)	1.237 (2)	1.254 (4)	1.235 (6)
N5−O2	1.256 (2)	1.244 (6)	1.260 (3)	1.276 (2)	1.260 (4)	1.246 (5)
N7−O3	1.242 (3)	1.266 (4)	1.246 (3)	1.242 (1)	1.282 (4)	1.245 (5)
N7−O4	1.254 (3)	1.235 (4)	1.262 (3)	1.259 (2)	1.260 (4)	1.251 (5)

dx.doi.org/10.1021/ja310384y | J. Am. Chem. Soc. 2012, 134, 20827−20836

bis(nitroimido)-1,2,3-triazolate anion is too large for the program to handle (>14 VB orbitals), so one nitroimide group was replaced with an *N*-oxide as an "approximate replacement"; however, the higher electronegativity of the oxygen atom vs a nitrogen was believed to favor the resonance forms with increased negative charge on the oxide vs the ring. Figure 12 illustrates the nine resonance forms which were calculated.

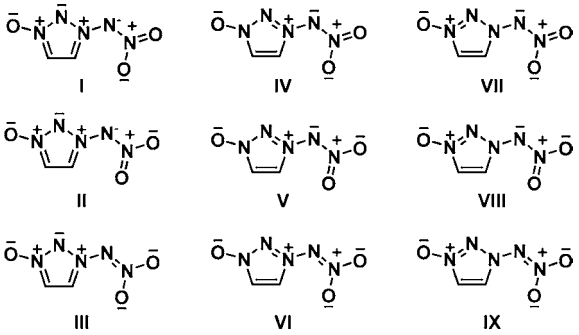

Figure 12. Valence bond resonance forms.

The calculated Hiberty Weights (percentage contribution of each resonance form) is 1.1%, 0%, 0%, 90.8%, 1.0%, 0.1%, 6.9%, 0.2%, and 0% for I–IX, respectively. The first piece of information that is noteworthy is the insignificant contribution of the resonance forms III, VI, and IX, those containing a double bond between the nitrogen atoms of the nitroimide groups, in interesting contrast to the results in the crystallography section. The next interesting piece of information is that when each column of resonance forms is considered individually, the only difference down a column being the resonance differences within the nitroimide group, within the standard NO_2 group resonances there is a distinct favorability to I, IV, and VII over II, V, and VIII. A potential explanation for this is that when the adjacent proton on the ring is considered to be of partial positive charge resonance forms I, IV, and VII allow the negatively charged oxygen atom to approach this proton, allowing for a six-membered ring to be established. Structure IV is the highest contributing resonance form over I and VII. The major difference between these three is the location of anionic negative charge, after the cancelling of charges within zwitterionic groups such as *N*-oxide, nitro, and nitroimide, on the ring, on the ring oxygen atom, and on the nitrimide nitrogen, respectively. When we consider the higher electronegativity of oxygen compared to nitrogen, it is unsurprising that resonance form IV is the highest contributor. In the 1,3-bis(nitroimido)-1,2,3-triazolate anion, this resonance form is naturally not possible due to the lack of said oxygen atom, meaning that resonance forms analogous to I and VII would be of higher contribution. Despite I contributing less than VII, its contribution would not be insignificant when we go from the model system above to the actual 1,3-bis(nitroimido)-1,2,3-triazolate anion, illustrating that while it may not be the most favored resonance form it is a contributor.

Thermal Behavior. The thermal behavior of all prepared compounds (Table 3) was investigated by differential scanning calorimetry. Only one compound, triaminoguanidinium salt **8**, melts prior to decomposition. Generally energetic salts of the 1,3-bis(nitroimido)-1,2,3-triazolate anion are of high thermal stability, decomposing only above 180 °C, a general requirement of an any energetic prior to adaptation for practical use.

Table 3. Thermal Behavior of Nitrogen-Rich Salts

compound	T_m (°C)	T_{dec} (°C)
1	-	210
2	-	238
3	-	184
4	-	149
5	-	210
6	145	185

The only exception to this trend is the hydroxylammonium salt **5** which decomposes below 150 °C; however, this is often seen for hydroxylammonium salts of nitro compounds, such as the hydroxylammonium nitrotetrazolate-2-oxide. The most stable salt is the silver salt **3** which decomposes at almost 240 °C. The generally high thermal stability of all salts of the 1,3-bis(nitroimido)-1,2,3-triazolate anion is comparable to or slightly higher than other known nitroimides.[24] These stabilities are far higher than for *N*-nitrimino systems incapable of forming APNC systems such as 1-and 2-nitraminotetrazoles,[41] again supporting the use of APNC theory in the design of thermally stable energetic systems.

Heats of Formation. It is commonly accepted that heats of formation of energetic materials are calculated theoretically, and even superior results are achieved. The calculations were carried out using the Gaussian G09W (revision A.02) program package.[28] The heats of formation $\Delta_f H°(s)$ (Table 5) of the investigated compounds **1** and **4**–**8** (silver cannot be calculated by the CBS-4 M method) were calculated with the atomization method (eq 1) using room-temperature CBS-4 M electronic enthalpies summarized in Table 5.[42−44]

$$\Delta_f H°_{(g,M,298)} = H_{(Molecule,298)} - \sum H°_{(Atoms,298)} + \sum \Delta_f H°_{(Atoms,298)} \quad (1)$$

The calculated gas-phase enthalpies of formation $\Delta_f H°(g)$ (Table 4) were converted into the solid state enthalpies of formation ($\Delta H_m(s)$) by using the Jenkins and Glasser

Table 4. CBS-4M Calculation Results, Molecular Volumes Taken from X-ray Solution, and Calculated Lattice Enthalpies

M	$-H^{298}$ (au)[a]	$\Delta_f H°(g,M)$ (kJ mol^{-1})[b]	V_M (nm^3)[c]	ΔE_L, ΔH_L (kJ mol^{-1})[d]	Δn[e]
K^+	599.035967	487.7			
NH_4^+	56.796608	635.8			
Hx^+	131.863229	687.2			
Hy^+	112.030523	774.1			
TAG^+	371.197775	874.3			
IMY^-	760.415222	351.0			9
1		838.7[f]	0.197	581.4, 582.6	6.5
3		986.8[f]	0.188	513.9, 518.9	9
4		1038.2[f]	0.205	502.0, 507.0	9.5
5		1125.1[f]	0.210	498.6, 503.5	10
6		1225.3[f]	0.290	458.4, 463.3	14

[a]CBS-4 M calculated enthalpy at room temperature. [b]Calculated gas-phase heat of formation by the atomization equation. [c]Molecular volume of the molecular moiety in the crystal structure. [d]Lattice energy and lattice enthalpy calculated by Jenkins and Glasser equations. [e]Change of moles of gaseous components. [f]Gas-phase enthalpies of formation of the ionic compounds are taken as the respective sums of the noninteracting component ions.

dx.doi.org/10.1021/ja310384y | J. Am. Chem. Soc. 2012, 134, 20827−20836

Table 5. Energetic Properties and Detonation Parameters

	1	3	4	5	6	RDX
formula	$C_2H_2KN_7O_4$	$C_2H_6N_8O_4$	$C_2H_6N_8O_5$	$C_2H_7N_9O_4$	$C_3H_{11}N_{13}O_4$	$C_3H_6N_6O_6$
FW (g mol^{-1})	227.18	206.12	222.12	221.13	293.20	222.12
IS[a] (J)	1	1	1	5	>5	7.5
FS[b] (N)	20	20	20	6	20	120
ESD[c] (J)	0.020	0.800	0.200	0.100	0.200	0.2
N^d (%)	43.16	54.36	50.45	57.01	62.10	37.84
Ω^e (%)	−10.56	−23.28	−14.41	−25.32	−40.92	−21.61
$T_{Dec}{}^f$ (°C)	210	184	149	210	185	205
ρ^g (g cm^{-3})	1.922	1.829	1.804	1.749	1.683	1.858 (90 K)
$\Delta_f H_m{}^{\circ h}$ (kJ mol^{-1})	256.1	468.0	531.3	621.6	761.9	86.3
$\Delta_f U^{\circ i}$ (kJ kg^{-1})	1198.0	2378.1	2497.3	2922.6	2716.4	489.0
EXPLO5.05:						
$\Delta_{Ex}U^{\circ j}$(kJ kg^{-1})	9736[q]	6711	7342	7068	6109	6190
$T_{det}{}^k$ (K)	5552[q]	4454	4896	4610	3951	4232
$\rho_{CJ}{}^l$ (kbar)	319[p], 367[q]	399	407	376	326	380
$V_{Det}{}^m$ (m s^{-1})	8698[p], 8823[q]	9406	9426	9337	8954	8983
$V_o{}^n$ (L kg^{-1})	600[q]	805	793	828	841	734
$I_S{}^o$ (s)	300[q]	271	275	277	259	258

[a]BAM Drophammer. [b]BAM Impact. [c]Electrical Spark Sensitivity. [d]Nitrogen Content. [e]Oxygen Balance. [f]Decomposition temperature from DSC (5 °C min^{-1}). [g]Density from X-ray diffraction. [h]Calculated molar enthalpy of formation. [i]Energy of formation [j]Total energy of detonation. [k]Explosion temperature. [l]Detonation Pressure. [m]Detonation Velocity. [n]Volume of Detonation Products. [o]specific impulse using isobaric (60 bar) conditions. [p]Calculated by Dr. Betsy Rice with Cheetah 6. [q]Calculated with EXPLO5.06

equations for 1:1 salts.[45] The molecular volumes V_M were calculated from the X-ray structures to calculate the lattice energies (ΔE_L) and enthalpies (ΔH_L). Lastly, the molar standard enthalpies of formation ($\Delta_f H_m$) were used to calculate the molar solid state energies of formation (ΔU_m) (Table 5) according to eq 2.

$$\Delta U_m = \Delta H_m - \Delta nRT \quad (2)$$

(Δn being the change of moles of gaseous components).

Investigated salts **1** and **3**−**6** are all formed endothermically. Highly positive heats of formations are usually calculated for nitrogen-rich material, with a large number of N−N single bonds. Oxygen-rich energetic materials such as nitro carbons[46] have mostly negative enthalpies of formation. The lowest heat of formation was calculated for the potassium salt **1** (256 kJ mol^{-1}), the most positive one for triaminoguanidinium salt **6** (762 kJ mol^{-1}) showing the largest number of N−N single bonds followed by the hydrazinium salt **5** (622 kJ mol^{-1}), which is also remarkably high. With respect to one kilogram, hydrazinium salt **5** shows the highest value (2923 kJ kg^{-1}) because of its lower molecular mass in comparison to **6**.

Detonation Parameters. To evaluate the utility of new energetic materials, usually their performance characteristics are calculated by computer codes such as EXPLO5.05[47] or Cheetah.[48] In this manuscript the calculation of the most important detonation parameters as well as the specific impulse (at 60 bar rocket conditions) (Table 5) were performed with the program package EXPLO5.05 for the nitrogen-rich salts. Values for the potassium salt were generated with a beta version of EXPLO5.06 (Dr. M. Sućeska) and Cheetah 6 in cooperation with the army research laboratory. The EXPLO5.05 program is based on the chemical equilibrium, steady-state model of detonation and uses the Becker−Kistiakowsky−Wilson equation of state (BKW EOS) for gaseous detonation products and Cowan−Fickett's equation of state for solid carbon. The highest values in terms of detonation performance were observed for compounds **3** and **4** due to their highest density. Their calculated detonation velocity (9406 m s^{-1} (**3**) and 9426 m s^{-1}) but also pressure (399 kbar (**3**) and 407 kbar (**4**)) are much greater than that of RDX. **4** shows also a remarkable high energy of detonation (−7342 kJ mol^{-1}) which is ca. 20% larger than that of RDX. **3**−**5** show also very promising propulsion values (specific impulse >270 s) which indicates a potential use in e.g. triple base propellant mixtures.

Sensitivities. For initial safety testing, the impact, friction, and electrostatic discharge sensitivity tests of the prepared salts were carried out.[49,50] The impact sensitivity tests were carried out according to STANAG 4489[51] and were modified according to instruction[52] using a BAM (Bundesanstalt für Materialforschung[50]) drophammer.[53] The friction sensitivity tests were carried out according to STANAG 2287[54] and were modified according to instruction[55] using a BAM friction tester. When the impact sensitivities of all salts are considered, all except **5** and **6** are highly sensitive explosives, well in the range of primary explosives, while **5** and **6** are slightly less sensitive at 5 J and are classified as sensitive according the UN recommendations for the transportation of dangerous goods.[56] The friction sensitivities of **1**, **3**, **4**, and **6** are all 20 N, classifying them as very sensitive, while compounds **2** and **5** are 5 and 6 N, respectively, classifying them as extremely sensitive. The electrostatic sensitivities of all salts of nitrogen-rich cations **3**−**6** are greater than the human body can generate, making for safe laboratory handling. Compounds **1** and **2** are far more sensitive at only 20 mJ, a value easily achievable by the human body mandating extra care with handling. When the sensitivities of all compounds are regarded as a whole, the generalization can be made that energetic materials based on the 1,3-bis(nitroimido)-1,2,3-triazolate anion are highly sensitive, indicating that while alternating positive and negative charges in a system can contribute to high thermal stability as seen earlier, correlation toward mechanical sensitivities is less applicable, and as seen in other systems[57] a large chain of cantenated nitrogen atoms, as well as compounds with

increasingly balanced oxygen balances, can still be generalized[11] as highly sensitive.

CONCLUSIONS

It is possible to nitrate the 1,3-diamino-1,2,3-triazoliumtriazolium cation to the 1,3-bis(nitroimido)-1,2,3-triazolate anion, and many energetic salts can be formed through metathesis reactions. The molecular and crystal structures of the nitrogen-rich salts were determined for the first time. Multinuclear NMR, IR, and Raman spectroscopy proved useful for the characterization of these salts. Computational results in terms of Mulliken and NBO charges support this structure as possessing a resonance for containing a chain of nine atoms of alternating positive and negative charges extending over the anion, and valence bond calculations also suggest this resonance form as being a not-insignificant contributor. The experimentally determined high densities, calculated performances, and real thermal stabilities support the use of alternating positive and negative charges and *N*-nitroimides in the design of advanced energetic materials with desirable properties. Unfortunately, the mechanical sensitivities of these materials proved to be too high for practical use, illustrating that while the *N*-nitroimides are useful, other molecular features which reduce their sensitivity must be developed.

EXPERIMENTAL SECTION

All reagents and solvents were used as received (Sigma-Aldrich, Fluka, Acros Organics) if not stated otherwise. Diaminotriazolium nitrate was prepared according to our method.[58] Melting and decomposition points were measured with a Linseis PT10 DSC using heating rates of 5 °C min^{-1}, which were checked with a Büchi Melting Point B-450 apparatus. ^{1}H, ^{13}C, and ^{15}N NMR spectra were measured with a JEOL Eclipse 270, JEOL EX 400, or a JEOL Eclipse 400 instrument. All chemical shifts are quoted in parts per million relative to TMS (^{1}H, ^{13}C) or nitromethane (^{15}N). Infrared spectra were measured with a Perkin-Elmer Spektrum One FT-IR instrument. Raman spectra were measured with a Perkin-Elmer Spektrum 2000R NIR FT-Raman instrument equipped with a Nd:YAG laser (1064 nm). Elemental analyses were performed with a Netsch STA 429 simultaneous thermal analyzer. Sensitivity data were determined using a BAM drophammer and a BAM friction tester. The electrostatic sensitivity tests were carried out using an Electric Spark Tester ESD 2010 EN (OZM Research).

CAUTION! *All materials prepared are all energetic compounds with sensitivity to various stimuli. While we encountered no issues in the handling of these materials, proper protective measures (face shield, ear protection, body armor, Kevlar gloves, and earthened equipment) should be used at all times.*

Potassium 1,3-Di(nitroimido)-1,2,3-triazolate (1). To a solution of dried 1,3-diamino-1,2,3-triazolium nitrate (0.40 g, 2.47 mmol) in 100 mL of acetonitrile nitronium tetrafluoroborate (1.00 g, 7.53 mmol) was added slowly. The mixture was stirred at 0 °C for 30 min and then allowed to heat to RT over 30 min. The reaction was stopped by the addition of potassium acetate (6.00 g, 61.13 mmol), and the mixture was stirred overnight. The precipitate was filtered off and washed with 500 mL of acetonitrile, and half of the solvent was removed in vacuo. Benzene (500 mL) was added and removed in vacuo, and this process was repeated four times. Removal of the remaining solvent under reduced pressure and extraction of the residue with dry acetonitrile gave 0.32 g (1.81 mmol, 73%) of crude **1** after evaporation of acetonitrile. DSC (5 °C min^{-1}): 210 °C (dec), IR (cm^{-1}) $\tilde{\nu}$ = 3181 (m), 3167 (m), 3141 (m), 2418 (w), 2360 (m), 2341 (m), 1772 (w), 1696 (w), 1684 (w), 1635 (w), 1559 (m), 1520 (w), 1396 (s), 1364 (s), 1305 (s), 1280 (s), 1249 (m), 1181 (w), 1075 (s), 1058 (s), 1042 (s), 1012 (s), 918 (w), 864 (m), 857 (m), 802 (m), 771 (s), 720 (w), 687 (w); Raman (1064 nm) $\tilde{\nu}$ = 3169 (17), 3142 (15), 2938 (14), 1548 (11), 1519 (38), 1437 (15), 1410 (18), 1364 (65), 1252 (62), 1183 (15), 1077 (35), 1046 (26), 1009 (100), 923 (10), 870 (19), 803 (10), 775 (15), 735 (11), 722 (12), 697 (10), 661 (10), 637 (11), 603 (1), 494 (20), 461 (21), 440 (23), 407 (21), 379 (21), 325 (19); ^{1}H NMR (DMSO-d_6) δ (ppm) = 8.75 (d, 2H, C*H*); ^{13}C NMR (DMSO-d_6) δ (ppm) = 129.7 (s, 2C, CH); ^{15}N NMR (DMSO-d_6) δ (ppm) = −6.2 (s, 2N, N5, N7, calcd −12.9), −43.0 (s, 2N, N1, N3, calcd −53.1), −113.6 (s, 2N, N4, N6, calcd −106.2), −115.3 (s, 1N, N2, calcd −108.1); *m*/*z* (FAB+) 39.00 (K^+); *m*/*z* (FAB−) 188.02 ($C_2H_2N_7O_4^-$). EA ($C_2H_2N_7O_4K$, 227.12) calcd: C, 10.57; N, 43.16; H, 0.89. Found: C, 11.46; N, 41.98; H, 0.94. BAM impact: 1 J. BAM friction: 20 N. ESD: 20 mJ.

Silver 1,3-Di(nitroimido)-1,2,3-triazolate (2). To a solution of **1** (1.08 g, 4.76 mmol) in 30 mL of distilled water was added a solution of silver nitrate (0.81 g, 4.76 mmol) in 30 mL of distilled water. The precipitate was filtered off, and the remaining solvent in the filtrate was removed under reduced pressure, leaving 0.81 g (2.74 mmol, 58%) of **2**. DSC (5 °C min^{-1}): 238 °C (dec), IR (cm^{-1}) $\tilde{\nu}$ = 3718 (m), 3163 (m), 2710 (w), 2445 (w), 2360 (m), 2341 (m), 2249 (w), 1669 (w), 1540 (m), 1517 (m), 1448 (s), 1364 (m), 1319 (m), 1257 (s), 1244 (s), 1184 (s), 1174 (s), 1081 (s), 1062 (m), 1040 (m), 1000 (m), 993 (m), 888 (m), 865 (m), 795 (s), 768 (m), 763 (m), 743 (m), 720 (m), 659 (w). BAM impact: 2 J. BAM friction: 5 N. ESD: 20 mJ.

Ammonium 1,3-Di(nitroimido)-1,2,3-triazolate (3). To a suspension of **2** (0.27 g, 0.91 mmol) in 10 mL of distilled water was added a solution of ammonium chloride (0.05 g, 0.91 mmol) in 10 mL of distilled water. The mixture was heated to 80 °C for 3 h; the precipitate was filtered off; and the remaining solvent in the filtrate was removed under reduced pressure, leaving 0.13 g (0.65 mmol, 71%) of **3**. DSC (5 °C min^{-1}): 184 °C (dec), IR (cm^{-1}) $\tilde{\nu}$ = 3507 (w), 3214 (m), 3158 (s), 3137 (s), 3063 (m), 2841 (m), 2271 (w), 1720 (w), 1652 (w), 1516 (w), 1390 (s), 1361 (s), 1262 (s), 1247 (s), 1180 (s), 1073 (s), 1054 (m), 999 (m), 953 (w), 856 (m), 795 (m), 783 (m), 768 (s), 720 (m), 660 (w); Raman (1064 nm) $\tilde{\nu}$ = 3162 (12), 3141 (12), 1541 (9), 1517 (32), 1362 (63), 1323 (16), 1251 (63), 1181 (10), 1078 (35), 1046 (16), 1008 (100), 870 (16), 774 (7), 735 (6), 722 (8), 663 (5), 637 (5), 494 (6), 441 (7), 406 (7), 381 (8), 325 (15); ^{1}H NMR (DMSO-d_6) δ (ppm) = 8.75 (d, 2H, C*H*), 7.12 (s, broad, 4H, NH_4); ^{13}C NMR (DMSO-d_6) δ (ppm) = 129.7 (s, 2C, CH); *m*/*z* (FAB^+) 18.03 (NH_4^+); *m*/*z* (FAB^-) 188.02 ($C_2H_2N_7O_4^-$). EA ($C_2H_2N_7O_4NH_4$, 206.12) calcd: C, 11.65; N, 54.36; H, 2.93. Found: C, 11.58; N, 48.18; H, 2.80. BAM impact: 1 J. BAM friction: 20 N. ESD: 800 mJ.

Hydroxylammonium 1,3-Di(nitroimido)-1,2,3-triazolate (4). To a solution of **2** (0.26 g, 0.88 mmol) in 10 mL of distilled water was added a solution of hydroxylammonium chloride (0.09 g, 0.88 mmol) in 10 mL of distilled water. The precipitate was filtered off, and the remaining solvent in the filtrate was removed under reduced pressure, leaving 0.11 g (0.52 mmol, 69%) of **4** (beige powder). DSC (5 °C min^{-1}): 149 °C (dec), IR (cm^{-1}) $\tilde{\nu}$ = 3155 (m), 3145 (m), 3076 (m), 2909 (m), 2759 (m), 2691 (m), 1738 (w), 1624 (m), 1580 (w), 1546 (w), 1501 (m), 1430 (s), 1406 (s), 1371 (s), 1298 (s), 1264 (s), 1247 (s), 1192 (s), 1158 (s), 1076 (s), 1051 (m), 1008 (s), 867 (s), 791 (s), 768 (s), 723 (s), 698 (m), 660 (m); Raman (1064 nm) $\tilde{\nu}$ = 3160 (10), 3143 (9), 1669 (9), 1538 (12), 1428 (13), 1372 (44), 1331 (13), 1251 (52), 1188 (15), 1186 (25), 1056 (22), 1015 (100), 875 (12), 787 (9), 733 (11), 666 (9), 636 (9), 551 (9), 498 (10), 440 (12), 413 (11), 392 (11), 334 (18), 240 (17); ^{1}H NMR (DMSO-d_6) δ (ppm) = 9.93 (s, broad, 4H, NH_3OH), 8.74 (d, 2H, C*H*), ^{13}C NMR (DMSO-d_6) δ (ppm) = 129.7 (s, 2C, CH); *m*/*z* (FAB^+) 34.03 (NH_4O^+); *m*/*z* (FAB^-) 188.02 ($C_2H_2N_7O_4^-$). EA ($C_2H_2N_7O_4NH_4O$, 222.12) calcd: C, 10.81; N, 50.45; H, 2.72. Found: C, 11.30; N, 48.56; H, 2.66. BAM impact: 1 J. BAM friction: 20 N. ESD: 200 mJ.

Hydrazinium 1,3-Di(nitroimido)-1,2,3-triazolate (5). To a solution of **2** (0.62 g, 2.10 mmol) in 20 mL of distilled water was added a solution of hydrazinium bromide (0.24 g, 2.10 mmol) in 20 mL of distilled water. The precipitate was filtered off, and the remaining solvent in the filtrate was removed under reduced pressure, leaving 0.46 g (2.08 mmol, 99%) of **5**. DSC (5 °C min^{-1}): 210 °C (dec), IR (cm^{-1}) $\tilde{\nu}$ = 3451 (m), 3320 (s), 3240 (m), 3166 (s), 3145 (s), 3013 (s), 2934 (m), 2781 (m), 2707 (m), 2627 (s), 2506 (m),

2416 (m), 2274 (m), 2094 (w), 2026 (w), 1749 (w), 1691 (w), 1626 (m), 1582 (m), 1537 (m), 1509 (s), 1404 (s), 1385 (s), 1266 (s), 1245 (s), 1179 (s), 1085 (s), 1050 (s), 1003 (s), 978 (s), 856 (m), 838 (m), 785 (s), 760 (s), 727 (m); Raman (1064 nm) $\tilde{\nu}$ = 3282 (7), 3260 (7), 3152 (11), 2827 (7), 2794 (7), 2699 (6), 2458 (4), 1629 (11), 1509 (61), 1435 (13), 1338 (100), 1301 (30), 1249 (77), 1182 (9), 1091 (98), 1047 (47), 1005 (93), 857 (45), 788 (8), 763 (7), 748 (7), 729 (11), 632 (5), 650 (5), 536 (6), 530 (5), 434 (9), 389 (13), 351 (12), 301 (20); ^{1}H NMR (DMSO-d_6) δ (ppm) = 8.73 (d, 2H, C*H*), 7.00 (s, broad, 5H, $N_2H_5^+$), ^{13}C NMR (DMSO-d_6) δ (ppm) = 129.7 (s, 2C, CH); m/z (FAB$^+$) 33.05 ($H_5N_2^+$); m/z (FAB$^-$) 188.02 ($C_2H_2N_7O_4^-$). EA ($C_2H_2N_7O_4H_5N_2$, 221.14) calcd: C, 10.86; N, 57.01; H, 3.19. Found: C, 11.28; N, 51.59; H, 3.47. BAM impact: 5 J. BAM friction: 6 N. ESD: 100 mJ.

Triaminoguanidinium 1,3-Di(nitroimido)-1,2,3-triazolate (6). To a solution of **2** (0.69 g, 2.34 mmol) in 20 mL of distilled water was added a solution of triaminoguanidinium chloride (0.33 g, 2.34 mmol) in 50 mL of distilled water. The precipitate was filtered off, and the remaining solvent in the filtrate was removed under reduced pressure, leaving 0.65 g (2.22 mmol, 95%) of **6**. DSC (5 °C min^{-1}): 145 °C (mp), 185 °C (dec), IR (cm^{-1}) $\tilde{\nu}$ = 3446 (w), 3361 (m), 3345 (m), 3221 (s), 3176 (m), 3029 (w), 2797 (w), 2707 (w), 2401 (w), 2274 (w), 1912 (w), 1776 (w), 1678 (s), 1596 (w), 1546 (w), 1509 (w), 1422 (m), 1399 (s), 1358 (m), 1290 (s), 1259 (s), 1240 (s), 1195 (m), 1169 (m), 1158 (m), 1132 (m), 1070 (m), 1045 (w), 1001 (w), 958 (m), 926 (s), 868 (m), 789 (m), 770 (m), 726 (w), 713 (w); Raman (1064 nm) $\tilde{\nu}$ = 3398 (5), 3349 (10), 3280 (15), 3264 (20), 3241 (17), 3206 (13), 3176 (14), 3151 (13), 1681 (29), 1649 (29), 1542 (30), 1512 (46), 1456 (30), 1411 (31), 1358 (61), 1325 (37), 1241 (81), 1171 (32), 1139 (32), 1070 (64), 1048 (53), 1009 (100), 871 (41), 772 (30), 716 (31), 637 (33), 491 (29), 402 (34), 367 (35), 313 (33), 263 (37), 210 (47); ^{1}H NMR (DMSO-d_6) δ (ppm) = 8.75 (d, 2H, C*H*), 8.58 (t, broad, 3H, N*H*), 4.48 (d, broad, 6H, NH_2); ^{13}C NMR (DMSO-d_6) δ (ppm) = 129.7 (s, 2C, CH); m/z (FAB$^+$) 105 ($CH_9N_6^+$); m/z (FAB$^-$) 188.02 ($C_2H_2N_7O_4$). EA ($C_2H_2N_7O_4CH_9N_6$, 222.12) calcd: C, 12.29; N, 62.10, H, 3.78. Found: C, 12.76; N, 61.59; H, 3.59. BAM impact: >5 J. BAM friction: 20 N. ESD: 200 mJ.

■ ASSOCIATED CONTENT

Ⓢ Supporting Information

CIF files are available. This material is available free of charge via the Internet at http://pubs.acs.org.

■ AUTHOR INFORMATION

Corresponding Author

tmk@cup.uni-muenchen.de

Notes

The authors declare no competing financial interest.

■ ACKNOWLEDGMENTS

Financial support of this work by the Ludwig-Maximilian University of Munich (LMU), the U.S. Army Research Laboratory (ARL), the Armament Research, Development and Engineering Center (ARDEC), and the Office of Naval Research (ONR Global, title: "Synthesis and Characterization of New High Energy Dense Oxidizers (HEDO) - NICOP Effort") under contract nos. W911NF-09-2-0018 (ARL), W911NF-09-1-0120 (ARDEC), W011NF-09-1-0056 (ARDEC), and 10 WPSEED01-002/WP-1765 (SERDP) is gratefully acknowledged. The authors acknowledge collaborations with Dr. Mila Krupka (OZM Research, Czech Republic) in the development of new testing and evaluation methods for energetic materials and with Dr. Muhamed Sucesca (Brodarski Institute, Croatia) in the development of new computational codes to predict the detonation and propulsion parameters of novel explosives. We are indebted to and thank Drs. Betsy M. Rice and Brad Forch (ARL, Aberdeen, Proving Ground, MD) and Mr. Gary Chen (ARDEC, Picatinny Arsenal, NJ) for the Cheetah calculation and many inspired discussions and support of our work. Prof. Jürgen Evers is thanked for obtaining the synchrotron measurements. Last but not least the authors thank Mr. St. Huber for the sensitivity measurements.

■ REFERENCES

(1) Zhang, M.-X.; Eaton, P. E.; Gilardi, R. *Angew. Chem., Int. Ed.* **2000**, *39*, 401−404.
(2) Tao, G.-H.; Twamley, B.; Shreeve, J. M. *J. Mater. Chem.* **2009**, *19*, 5850−5854.
(3) Klapötke, T. M.; Stierstorfer, J. *J. Am. Chem. Soc.* **2009**, *131*, 1122−1134.
(4) Gao, H.; Shreeve, J. M. *Chem. Rev.* **2011**, *111*, 7377−7436.
(5) Wang, R.; Xu, H.; Guo, Y.; Sa, R.; Shreeve, J. M. *J. Am. Chem. Soc.* **2010**, *132*, 11904−11905.
(6) Binnikov, A. N.; Kulikov, A. S.; Makhov, N. N.; Orchinnikov, I. V.; Pivina, T. *30th International Annual Conference of ICT*; Karlsruhe: Germany, June 29-July 2, 1999; pp 58/1−58/10.
(7) Huynh, M. H. V.; Hiskey, M. A.; Meyer, T. J.; Wetzler, M. *Proc. Natl. Acad. Sci. U.S.A.* **2006**, *103*, 5409−5412.
(8) Evers, J.; Klapötke, T. M.; Mayer, P.; Oehlinger, G.; Welch, J. *Inorg. Chem.* **2006**, *45*, 4996−5007.
(9) Lukin, K.; Li, J.; Gilardi, R.; Eaton, P. E. *Angew. Chem., Int. Ed.* **2000**, *35*, 864−866.
(10) Li, Y.-C.; Qi, C.; Li, S.-H.; Zhang, H.-J.; Sun, C.-H.; Yu, Y.-Z.; Pang, S.-P. *J. Am. Chem. Soc.* **2010**, *132*, 12172−12173.
(11) Adolph, H. G.; Holden, J. R.; Cichra, D. A. Relationships between the impact sensitivity of high energy compounds and some molecular properties which determine their performance; N, M, and ρ_0. *Report No A101203*; Naval Surface Weapons Center, Dahlgren, Virgnina, 1981.
(12) Carlqvist, P.; Ostmark, H.; Brinck, T. *J. Phys. Chem. A* **2004**, *108*, 7463−7467.
(13) Eaton, P. E.; Zhang, M.-X.; Gilardi, R.; Gelber, N.; Iyer, S.; Surapeneni, R. *Propellants, Explos., Pyrotech.* **2001**, *27*, 1−6.
(14) Inagake, S.; Goto, N. *J. Am. Chem. Soc.* **1987**, *109*, 3234−3240.
(15) Noyman, M.; Zilberg, S.; Haas, Y. *J. Phys. Chem. A* **2009**, *113*, 7376−7382.
(16) Tartakovsky, V. A. *Mater. Res. Soc. Symp. Proc.* **1996**, *418*, 15−24.
(17) Kalinin, A. V.; Apasov, E. T.; Ioffe, S. L.; Tartakovsky, V. A. *Bull. Acad. Sci. USSR, Div. Chem. Sci.* **1991**, *40*, 988.
(18) Kaihoh, T.; Itoh, T.; Yamagucha, K.; Ohsawa, A. *J. Chem. Soc., Chem. Commun.* **1988**, 1608−1609.
(19) Kaihoh, T.; Itoh, T.; Yamagucha, K.; Ohsawa, A. *J. Chem. Soc., Perkin Trans. 1* **1991**, 2045−2048.
(20) Churakov, A. M.; Tartakovsky, V. A. *Chem. Rev.* **2004**, *104*, 2601−2616.
(21) Rezchikova, K. I.; Churakov, A. M.; Burshtein, K. Y.; Shlyapochnikov, V. A.; Tartakovskii, V. A. *Mendeleev Commun.* **1997**, *7*, 174−175.
(22) Klapötke, T. M.; Piercey, D. G.; Stierstorfer, J.; Weyrauther, M. *Propellants, Explos., Pyrotech.* **2012**, *37*, 527−535.
(23) Shechter, H.; Venugopal, M.; Srinivasulu, D. Synthesis of 1,2,3,4-Tetrazine Di-N-Oxides, Pentazole Derivatives, Pentazine Poly-N-oxides and Nitroacetylenes. *Project 746566, Grant No FA 9550−40−1-0410*; USAF AFRL Arlington: VA, 2006.
(24) Epsztajn, J.; Katritzky, A. R.; Lunt, E.; Mitchell, J. W.; Roch, G. *J. Chem. Soc., Perkin Trans. 1* **1973**, 2622−2624.
(25) Myasnikov, V. A.; Vyazkov, V. A.; Yudin, I. L.; Shitov, O. P.; Tartakovskii, V. A. *Izv. Akad. Nauk SSSR, Ser. Khim.* **1991**, *5*, 1239.
(26) Churakov, A. M.; Ioffe, S. L.; Tartakovskii, V. A. *Mendeleev Commun.* **1996**, *6*, 20−22.
(27) Shitov, O. P.; Vyazkov, V. A.; Tartakovskii, V. A. *Izv. Akad. Nauk SSSR, Ser. Khim* **1989**, *11*, 2654−2655.

(28) Frisch, M. J.; Trucks, G. W.; Schlegel, H. B.; Scuseria, G. E.; Robb, M. A.; Cheeseman, J. R.; Scalmani, G.; Barone, V.; Mennucci, B.; Petersson, G. A.; Nakatsuji, H.; Caricato, M.; Li, X.; Hratchian, H. P.; Izmaylov, A. F.; Bloino, J.; Zheng, G.; Sonnenberg, J. L.; Hada, M.; Ehara, M.; Toyota, K.; Fukuda, R.; Hasegawa, J.; Ishida, M.; Nakajima, T.; Honda, Y.; Kitao, O.; Nakai, H.; Vreven, T.; Montgomery, Jr., J. A.; Peralta, J. E.; Ogliaro, F.; Bearpark, M.; Heyd, J. J.; Brothers, E.; Kudin, K. N.; Staroverov, V. N.; Kobayashi, R.; Normand, J.; Raghavachari, K.; Rendell, A.; Burant, J. C.; Iyengar, S. S.; Tomasi, J.; Cossi, M.; Rega, N.; Millam, J. M.; Klene, M.; Knox, J. E.; Cross, J. B.; Bakken, V.; Adamo, C.; Jaramillo, J.; Gomperts, R.; Stratmann, R. E.; Yazyev, O.; Austin, A. J.; Cammi, R.; Pomelli, C.; Ochterski, J. W.; Martin, R. L.; Morokuma, K.; Zakrzewski, V. G.; Voth, G. A.; Salvador, P.; Dannenberg, J. J.; Dapprich, S.; Daniels, A. D.; Farkas, Ö.; Foresman, J. B.; Ortiz, J. V.; Cioslowski, J.; Fox, D. J. *Gaussian 09*, Revision A2; Gaussian, Inc.: Wallingford CT, 2009.
(29) Becke, A. D. *J. Chem. Phys.* **1993**, *98*, 5648−5652.
(30) Lee, C.; Yang, W.; Parr, R. G. *Phys. Rev. B* **1988**, *37*, 785−789.
(31) Woon, D. E.; Dunning, T. H., Jr. *J. Chem. Phys.* **1993**, *98*, 1358−1371.
(32) Kendall, R. A.; Dunning, T. H., Jr.; Harrison, R. J. *J. Chem. Phys.* **1992**, *96*, 6796−6806.
(33) Dunning, T. H., Jr. *J. Chem. Phys.* **1989**, *90*, 1007−1023.
(34) Peterson, K. A.; Woon, D. E.; Dunning, T. H., Jr. *J. Chem. Phys.* **1994**, *100*, 7410−7415.
(35) Klapötke, T. M.; Stierstorfer, J.; Wallek, A. U. *Chem. Mater.* **2008**, *20*, 4519−4530.
(36) Arriau, J.; Deschamps, J. *Tetrahedron Lett.* **1974**, *44*, 3865−3868.
(37) Huang, Y.; Gao, H.; Twamley, B.; Shreeve, J. M. *Eur. J. Inorg. Chem.* **2008**, 2560−2568.
(38) Laus, G.; Kahlenberg, V.; Toebbens, D. M.; Jetti, R. K. R.; Greisser, U. J.; Schuetz, J.; Kristeva, E.; Wurst, K.; Schottenberger, H. *Cryst. Growth Des.* **2006**, *6*, 404−410.
(39) Li, J.: Duke, B.; McWeeny, R. *VB2000*, version 2.1; SciNet Technologies: San Diego, CA, 2009.
(40) Li, J.; McWeeny, R. *Int. J. Quantum Chem.* **2002**, *89*, 208−216.
(41) Ilyushin, M. A.; Terpigorev, A. N.; Tselinskii, I. V. *Russ. J. Gen. Chem.* **1999**, *69*, 1654−1657.
(42) Ochterski, J. W.; Petersson, G. A.; Montgomery, J. A., Jr. *J. Chem. Phys.* **1996**, *104*, 2598.
(43) Montgomery, J. A., Jr.; Frisch, M. J.; Ochterski, J. W.; Petersson, G. A. *J. Chem. Phys.* **2000**, *112*, 6532.
(44) (a) Curtiss, L. A.; Raghavachari, K.; Redfern, P. C.; Pople, J. A. *J. Chem. Phys.* **1997**, *106*, 1063. (b) Byrd, E. F. C.; Rice, B. M. *J. Phys. Chem. A* **2006**, *110*, 1005−1013. (c) Rice, B. M.; Pai, S. V.; Hare, J. *Combust. Flame* **1999**, *118*, 445−458.
(45) (a) Jenkins, H. D. B.; Roobottom, H. K.; Passmore, J.; Glasser, L. *Inorg. Chem.* **1999**, *38*, 3609−3620. (b) Jenkins, H. D. B.; Tudela, D.; Glasser, L. *Inorg. Chem.* **2002**, *41*, 2364−2367.
(46) Nielsen, A. T. *Nitrocarbons*, 1st ed.; Wiley-VCH: Weinheim, 1995.
(47) (a) Sućeska, M. *Mater. Sci. Forum* **2004**, *465*−*466*, 325−330. (b) Sućeska, M. *Propellants, Explos., Pyrotech.* **1999**, *24*, 280−285. (c) Suceska, M. *Propellants, Explos., Pyrotech.* **1991**, *16*, 197−202.
(48) Lu, J. P. *Evaluation of the Thermochemical Code—CHEETAH 2.0 for Modelling Explosives Performance*; DSTO Aeronautical and Maritime Research Laboratory: Edinburgh, 2001.
(49) Sućeska, M. *Test Methods for Explosives*; Springer: New York, 1995; p 21 (impact), p 27 (friction).
(50) www.bam.de.
(51) NATO standardization agreement (STANAG) on explosives, impact sensitivity tests, no. 4489, Ed. 1, Sept. 17, 1999.
(52) WIWEB-Standardarbeitsanweisung 4−5.1.02, Ermittlung der Explosionsgefährlichkeit, hier der Schlagempfindlichkeit mit dem Fallhammer, Nov. 8, 2002.
(53) http://www.reichel-partner.de.
(54) NATO standardization agreement (STANAG) on explosives, friction sensitivity tests, no. 4487, Ed. 1, Aug. 22, 2002.
(55) WIWEB-Standardarbeitsanweisung 4−5.1.03, Ermittlung der Explosionsgefährlichkeit oder der Reibeempfindlichkeit mit dem Reibeapparat, Nov. 8, 2002.
(56) Impact: Insensitive > 40 J, less sensitive ≥ 35 J, sensitive ≥ 4 J, very sensitive ≤ 3 J; Friction Insensitive > 360 N, less sensitive = 360 N, sensitive < 360 N a. > 80N, very sensitive ≤ 80 N, extremely sensitive ≤ 10 N. According to the UN Recommendations on the Transport of Dangerous Goods.
(57) Klapötke, T. M.; Piercey, D. G. *Inorg. Chem.* **2011**, *50*, 2732−2734.
(58) Klapötke, T. M.; Piercey, D. G.; Stierstorfer, J. *Eur. J. Inorg. Chem.* **2012**, DOI: 10.1002/ejic.201201237.